A Smooth Control Law for Graceful Motion of Differential Wheeled Mobile Robots in 2D Environment

Jong Jin Park and Benjamin Kuipers

Abstract— **Although recent progress in 2D mobile robot navigation has been significant, the great majority of existing work focuses only on ensuring that the robot reaches its goal. But to make autonomous navigation truly successful, the 'quality' of planned motion is important as well. Here, we develop and analyze a pose-following kinematic control law applicable to unicycle-type robots, such that the robot can generate intuitive, fast, smooth, and comfortable trajectories.**

The Lyapunov-based feedback control law is derived via singular perturbation. It is made up of three components: (i) egocentric polar coordinates with respect to an observer on the vehicle, (ii) a slow subsystem which describes the position of the vehicle, where the reference heading is obtained via state feedback, and (iii) a fast subsystem which describes the steering of the vehicle, where the vehicle heading is exponentially stabilized to the obtained reference heading. The resulting path is a smooth and intuitive curve, globally converging to an arbitrary target pose without singularities, from any given initial pose.

Furthermore, we present a simple path following strategy based on the proposed control law to satisfy arbitrary velocity, acceleration and jerk bounds imposed by the user. Such requirements are important to any autonomous vehicle so as to avoid actuator overload and to make the path physically realizable, and they are critical for applications like autonomous wheelchairs where passengers can be physically fragile.

I. INTRODUCTION

Planar motion control is a fundamental problem for any autonomous mobile platform, and it has been a very active area of research for the past few decades with a large body of existing literature. Many existing approaches for planar motion control involves target tracking, with targets being positional waypoints or attached to a predefined pathway [3].

Waypoint-following control is common in the fields of aerospace and naval sciences, where orientation of a vehicle arriving at a desired target carry less importance as in the case of missile guidance or control of surface vessels [9], [10]. The method is simple and intuitive, and it can be robust to disturbances since there is no associated deviation-from-path error. But with this method, smooth transitions between waypoints is an inherent problem; the orientation and velocity at a given location significantly influence subsequent motion and control effort, but positional waypoints do not provide constraints on those quantities.

Path-following control addresses this issue by first designing the entire pathway and then making the system converge to the path [16], [17], [18], [19]. With control over the design of the pathway, tasks which can be difficult to solve with waypoint-following such as static obstacle avoidance can readily be solved. However, this approach does require accurate and explicit path planning, and in general it does not work well with dynamic obstacles like pedestrians. Also, with current methods it is not clear how to make motion along the path smooth and comfortable, i.e. with bounded velocity, acceleration, and jerk. The situation can be more problematic when the path is designed independently of vehicle dynamics, which is typical of path design by parametric curves such as B-splines.

In terms of comfortable motion, other popular classical methods such as VFH [11] or DWA [12] are also not suitable. Since these methods are completely reactive [1], in the sense that the desired velocity is calculated based on the information at a single time step, the resulting acceleration and jerk can be arbitrarily large. Likewise, the great majority of existing control methods assumes ideal actuators, i.e. arbitrarily large velocity or torque can be generated instantly [7]. Such an assumption fails to sufficiently account for the robot dynamics, which in turn can lead to failure in navigation [4].

The issue becomes even more critical in the case of an autonomous wheelchair, which is the primary target application of the control methods proposed in this paper. An intelligent wheelchair which is capable of autonomous and safe navigation between distinct points in an environment can provide a necessary level of motor assistance to individuals suffering from physical or mental disabilities. But control methods which do not limit the velocity, acceleration and jerk are clearly not suitable for wheelchairs since high acceleration can harm passengers even without a collision, in addition to being uncomfortable. Furthermore, we also stress that the path should be intuitive (appear natural) enough to be acceptable to human passengers.[1]

Thus we require the motion of the robot to be *graceful*. We use the qualitative term *graceful* as introduced by [1] to refer to a motion visibly safe, comfortable, fast and intuitive. To be safe and comfortable, a motion needs to be smooth with bounded velocity, acceleration and jerk.

Only limited attention has been paid to this subject. In [7], a path following control law is modified to limit actuator

This work has taken place in the Intelligent Robotics Lab in the Computer Science and Engineering Division of the University of Michigan. Research of the Intelligent Robotics lab is supported in part by grants from the National Science Foundation (CPS-0931474), and from the TEMA-Toyota Technical Center.

J. Park is with the Department of Mechanical Engineering, University of Michigan, Ann Arbor, MI 48105, USA `jongjinp@umich.edu`

B. Kuipers is with Faculty of Computer Science and Engineering, University of Michigan, Ann Arbor, MI 48105, USA `kuipers@umich.edu`

[1] These are general requirements to all autonomous vehicles intended to carry human passengers, but the issues are more pronounced for wheelchairs.

velocity. The approach in [1] also builds upon an existing path following control law [17] and achieves bounds in angular velocity and angular acceleration by adjusting linear velocity according to path curvature. In [2], the trajectory and associated control signal is fully generated via numerical optimization with a cost function which provides graceful motion, but without a closed-form control law.

In this paper, we take a different approach to achieve graceful motion. We first show that with a natural choice of a coordinate system, a simple and robust kinematic control law can be found via singular perturbation [14], which guides a wheelchair from a given pose (position and orientation), guaranteeing convergence to an arbitrary motion target (a prescribed position, orientation, and linear velocity), following a smooth, intuitive curve. Then we show that this closed-form control law makes it possible to design a set of motion targets to guide the robot toward a specified goal with bounded velocity, acceleration and jerk.

II. KINEMATIC EQUATIONS

It is well known that differential drive cart and simple cars can be modeled as a simple unicycle [15]. Consider a vehicle described by the unicycle model implemented with two independently driven parallel wheels such that linear velocity and angular velocity can be controlled independently. The vehicle is underactuated in the sense that the linear velocity of the vehicle is always aligned with the orientation of the vehicle (i.e. the vehicle cannot move sideways).

We adopt a polar coordinate system to describe the vehicle kinematics. One reason is that it is simply not possible to find a smooth state feedback control law using Cartesian representation of unicycles (Brockett's result, [20]). But more importantly, we try to identify and follow how human drivers observe and describe a target, such that the derived control law using the coordinate system can produce motion which appears natural to human passengers.

Suppose an observer, or a sensor, is situated on a vehicle and fixating at a target T at a distance r away from the vehicle. Let $\theta \in (-\pi, \pi]$ be the orientation of T with respect to the line of sight from the observer to the target. And let $\delta \in (-\pi, \pi]$ be the orientation of the vehicle heading with respect to the line of sight, as shown in Fig. 1.

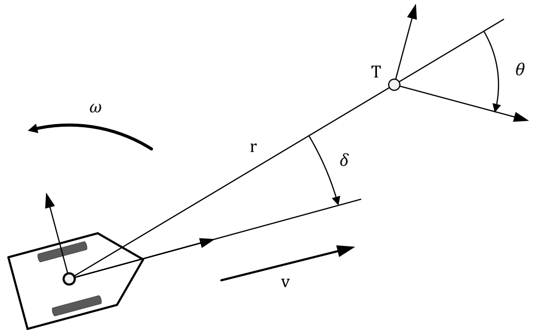

Fig. 1. Egocentric polar coordinate system with respect to the observer. Here, both θ and δ have negative values.

Then, it is easy to show that the vehicle kinematics can be written as

$$\begin{pmatrix} \dot{r} \\ \dot{\theta} \\ \dot{\delta} \end{pmatrix} = \begin{pmatrix} -v\cos\delta \\ \frac{v}{r}\sin\delta \\ \frac{v}{r}\sin\delta + \omega \end{pmatrix} \tag{1}$$

where v and ω are linear and angular velocity of the vehicle, respectively. A nearly identical set of state equations can be found in [5], but wherein the coordinates are defined with respect to the target rather than the observer.

III. KINEMATIC CONTROL LAW

From the previous section, we have $(r, \theta, \delta)^T$ as our coordinates of error space where the control problem is developed and solved. The control problem of moving a vehicle from any given initial pose to a target pose T becomes the problem of bringing $(r, \theta, \delta)^T$ to the origin. We treat velocity commands v and ω as the control variables, i.e. the controller is developed at kinematic control level.

To begin, let us assume v is some nonzero positive (not necessarily constant) and ω is the only control signal. Then from (1), it can be seen that the control signal ω only affects the state δ, and $(r, \theta)^T$ are determined via δ. Also observe that r and θ completely describes the position of the vehicle, and δ corresponds to steering the vehicle. Thus we can decompose the system (1) into two parts as follows.

$$\begin{pmatrix} \dot{r} \\ \dot{\theta} \end{pmatrix} = \begin{pmatrix} -v\cos\delta \\ \frac{v}{r}\sin\delta \end{pmatrix} \tag{2}$$

$$\dot{\delta} = \frac{v}{r}\sin\delta + \omega \tag{3}$$

This decomposed structure of the system motivates a control strategy via singular perturbation, or two-time scale decomposition. The idea is to find (a) virtual control δ (vehicle heading) which steers the subsystem (2) (vehicle position) to the origin, and (b) real control ω which render the dynamics of the subsystem (3) sufficiently faster than the subsystem (2) and stabilizes δ quickly to a desired virtual control, such that (2) becomes a slow subsystem and (3) becomes a fast subsystem in a singularly perturbed form. Note that this process is analogous to a human driver controlling the steering wheel (fast subsystem) to drive the vehicle (slow subsystem) to a desired pose in space.

A. Slow Subsystem and the Reference Heading

For the slow subsystem (2), consider a simple Lyapunov function candidate

$$V = \frac{1}{2}(r^2 + \theta^2) \tag{4}$$

Let the virtual control δ for the slow subsystem be

$$\delta = \arctan(-k_1\theta) \tag{5}$$

where k_1 is a positive constant. Then trajectory of (2) along (5) can be written as

$$\begin{pmatrix} \dot{r} \\ \dot{\theta} \end{pmatrix} = \begin{pmatrix} -v\cos(\arctan(-k_1\theta)) \\ \frac{v}{r}\sin(\arctan(-k_1\theta)) \end{pmatrix} \tag{6}$$

Then the derivative of V along (6) becomes

$$\begin{aligned}\dot{V} &= r\dot{r} + \theta\dot{\theta} \\ &= -rv\cos\left(\arctan\left(-k_1\theta\right)\right) + \frac{v}{r}\,\theta\,\sin\left(\arctan\left(-k_1\theta\right)\right)\end{aligned}$$

which is strictly less than zero everywhere other than $r = 0$, since

$$\begin{aligned}\cos\left(\arctan\left(-k_1\theta\right)\right) &> 0, \qquad {}^{\forall}\theta \in (-\pi, \pi] \\ sgn(\arctan\left(-k_1\theta\right)) &= -sgn(\theta)\end{aligned}$$

and $r \geq 0$ and $v > 0$ by definition. Thus the virtual control (5) steers the system (2) from arbitrary initial position toward the origin. Note that since $\arctan(\cdot)$ is a smooth function and $\arctan(0) = 0$, we have $\delta \to 0$ as $\theta \to 0$ from (5), which implies the overall states $(r, \theta, \delta)^T$ also approaches the origin. Furthermore, by choosing v to remove the singularity in r (e.g., by setting $v = f(r)$ such that $v = k_3 r$ in some neighborhood around $r = 0$, where k_3 is a positive constant), we can guarantee that the origin is globally asymptotically stable.

The virtual control (5) can be understood as the reference heading of the vehicle obtained from current state θ. It characterizes a slow manifold (Fig. 2) that the fast dynamics of the vehicle heading will converge to. The simple equation (5) enables us to design a set of reasonable and intuitive global manifolds[2] leading to a given target, in the sense that the error coordinates r and θ always decrease smoothly.

Geometrically, the path given by the virtual control is the well-known Archimedean spiral [13]. From (6), we have

$$\begin{aligned}\frac{\dot{\theta}}{\dot{r}} &= k_1\frac{\theta}{r} \\ \therefore\ \frac{\dot{\theta}}{\theta} &= k_1\frac{\dot{r}}{r} \qquad (7)\end{aligned}$$

which implies that k_1 is the ratio of the rate of change in θ to the rate of change in r. The solution to (7) is

$$r = a\,\theta^{\frac{1}{k_1}} \qquad (8)$$

with scaling factor $a = r_0/\theta_0^{\frac{1}{k_1}}$, where r_0 and θ_0 are initial conditions.

B. Fast Subsystem and Closed-Loop Steering

Now we develop a feedback control law for the steering. Let z denote the difference between the actual state δ and the desired property $\arctan(-k_1\theta)$, such that

$$z \equiv \delta - \arctan\left(-k_1\theta\right) \qquad (9)$$

Calculation of $\dot{z}$ is straightforward. From (3) and (6),

$$\begin{aligned}\dot{z} &= \dot{\delta} - \frac{d}{dt}\arctan\left(-k_1\theta\right) \\ &= \dot{\theta} + \omega - \frac{-k_1}{1+(k_1\theta)^2}\dot{\theta} \\ &= \left(1 + \frac{k_1}{1+(k_1\theta)^2}\right)\frac{v}{r}\sin\left(z + \arctan\left(-k_1\theta\right)\right) + \omega\end{aligned}$$

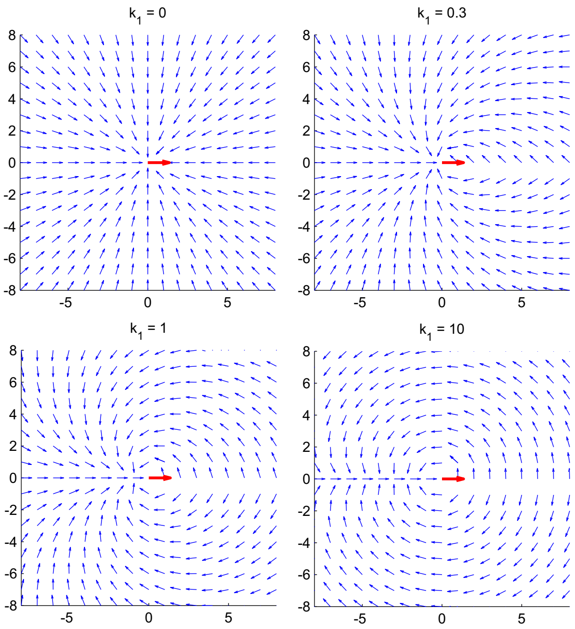

Fig. 2. Design of slow manifold with k_1, which is the ratio of the rate of change in θ to the rate of change in r. Target (red) is shown as a larger arrow at the center. Note $k_1 = 0$ reduces the controller to pure waypoint-following, while $k_1 \gg 0$ offers extreme scenario of pose-following where θ is reduced much faster than r.

Now, let ω be

$$\omega = -\frac{v}{r}\left[k_2\,z + \left(1 + \frac{k_1}{1+(k_1\theta)^2}\right)\sin\left(z + \arctan\left(-k_1\theta\right)\right)\right] \qquad (10)$$

with nonzero positive gain k_2, so that

$$\dot{z} = -k_2\frac{v}{r}z \qquad (11)$$

Furthermore, let $\tau \equiv \frac{r}{v}$, which is the minimum time needed for the vehicle to reach a goal, which is a relevant time scale for slow dynamics of (2). Then, with $k_2 \gg 1$, we can treat $\epsilon \equiv \frac{\tau}{k_2}$ as a small time scale which ensures the fast dynamics to indeed be faster than the slow dynamics. That is, we have

$$\epsilon\,\dot{z} = -z \qquad (12)$$

which is globally exponentially stable, and ensures that the fast subsystem quickly decays to the slow manifold. Numerical evaluation of the decay is shown in Fig. 3.

In the original coordinates, the control law (10) can be written as

$$\omega = -\frac{v}{r}\left[k_2(\delta - \arctan\left(-k_1\theta\right)) + \left(1 + \frac{k_1}{1+(k_1\theta)^2}\right)\sin\delta\right] \qquad (13)$$

Thus, (13) is our control law for ω. Recall that we placed no restriction on v, other than to be nonzero positive.[3] That is, we essentially have v as a free variable.

[2] Note that it is the manifold, not a path, that is being planned here. In path-following, the controller will try to steer the vehicle back to a specified path when it deviates. But here, a new vehicle heading is simply recalculated with feedback, from manifold given by (5).

[3] To admit negative linear velocity, we can simply flip the orientation of the vehicle and the target simultaneously when the sign of v changes.

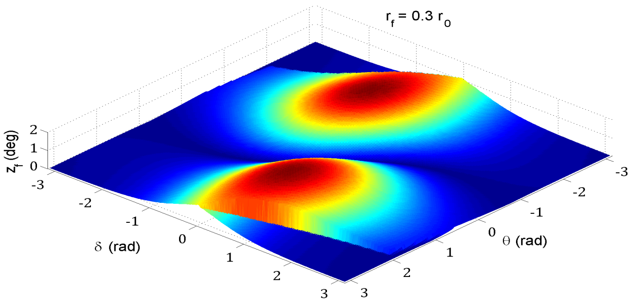

Fig. 3. Exponential decay of the heading error z under the control law (13) with $k_1 = 1$ and $k_2 = 3$. The vehicle starts with initial conditions of some nonzero $r_0 > 0$, $\theta \in (\pi, -\pi]$, and $\delta \in (-\pi, \pi]$, where $\max(z_0) \simeq 250$ (deg). Plot shows the value of z at $r_f = 0.3\, r_0$ against various values of initial conditions of θ and δ. The maximum value of $z_f < 1.9$ (deg).

Also, ω is a linear function of v. Specifically, we have $\omega = \kappa(r, \theta, \delta)\, v$, where κ is the curvature of the path resulting from the proposed control law. Curvature of a path of a vehicle moving on a plane with linear velocity v and angular velocity ω is simply ω / v. We can write

$$\kappa = -\frac{1}{r}\left[\, k_2(\delta - \arctan(-k_1\theta)) + (1 + \frac{k_1}{1+(k_1\theta)^2})\sin\delta\,\right] \tag{14}$$

which implies that the shape of the path is not influenced by the choice of v.

Recall from the previous subsection that asymptotic convergence to the target depends on the choice of v. Namely, the origin is globally asymptotically stable if and only if $v \to 0$ as $r \to 0$. With such a choice, the control law is a solution to a so-called parking problem, stabilizing the vehicle at a specific target pose.

The control law is also a solution to what can be called the passing problem: as the control law also guarantees that (r, θ, δ) approaches the origin with arbitrary nonzero positive v, the vehicle can arrive and pass through specific pose in space. It implies a straightforward implementation for a scenario following a path or trajectory (given by series of poses).

Fig. 4 shows some example trajectories of a unicycle under the proposed control law. The vehicle can approach arbitrary motion targets with a smooth and intuitive curve.

Fig. 4 shows example trajectories of a unicycle with the proposed control law, with constants $k_1 = 1$ and $k_2 = 3$. The vehicle can approach arbitrary motion targets with a smooth and intuitive curve. Fig. 5 shows trajectories to the same motion targets, but with constants $k_1 = 1$ and $k_2 = 10$.

IV. PATH FOLLOWING VIA STATIC MOTION TARGETS

In the previous section, we have established the convergence properties of the smooth control law (13). Now we build upon the result and show how graceful motion can be achieved, using a series of sparsely placed target poses as a path instruction. That is, a user instructs a sparse series of target poses, and the robot will generate full motor commands which guarantees graceful navigation via the targets[4]. When unacceptable target instructions (involving collisions, etc.) are given, they can easily be detected and rejected via model predictive simulation.

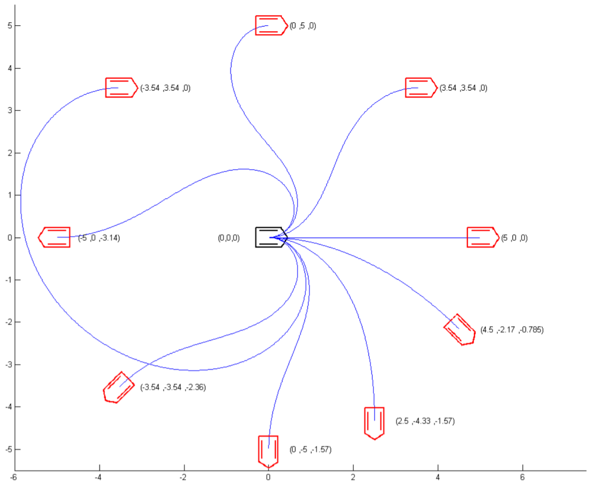

Fig. 4. Example trajectories of a unicycle with the proposed control law, with constants $k_1 = 1$ and $k_2 = 3$. Initial pose is marked black at the center, and target poses are colored red. The coordinates of the poses are given as (x, y, θ_P) where θ_P is the orientation of the vehicle with respect to reference frame.

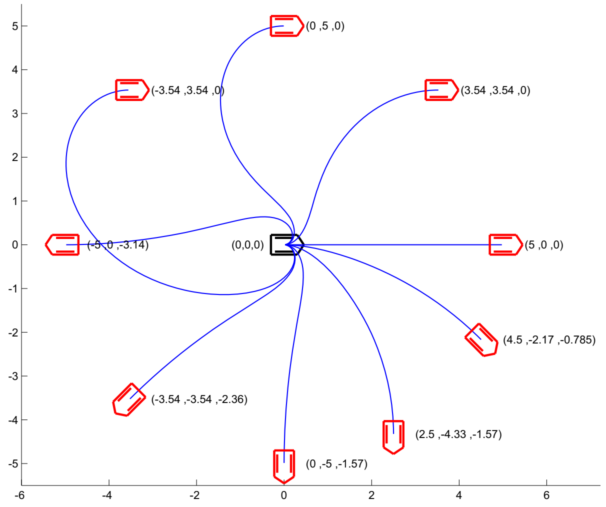

Fig. 5. Example trajectories of a unicycle with the proposed control law, with constants $k_1 = 1$ and $k_2 = 10$. Note that the vehicle converge to the slow manifold more quickly with higher value of k_2.

A. Simple Linear Velocity Selector

In a path following scenario, perhaps the simplest approach for smooth navigation would be to adjust linear velocity of the vehicle as a function of path curvature. Note that the task becomes particularly easy with the proposed control law, since path curvature can be obtained directly from feedback (14) and linear velocity v is a free variable.

Specifically, we require $v \to 0$ as $\kappa \to \infty$, and $v \to v_{\max}$ as $\kappa \to 0$, where $v_{\max}$ is imposed maximum linear velocity.

[4] We avoid the term 'waypoints' since it implies the instructions are given as positions. Here the instructions are given as target poses.

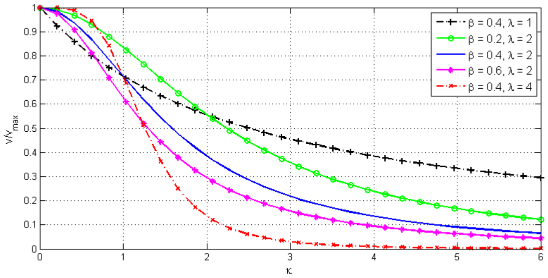

Fig. 6. Effect of design parameters β and λ on the curvature-based velocity rule (15) which has bell-shaped profile. Higher value of λ results in more sharply peaked curve, and higher value of β let the velocity drop more quickly as κ increases.

A practical solution (not optimized) which satisfies the requirements is

$$v(\kappa) = v(r,\theta,\delta) = \frac{v_{\max}}{1+\beta|\kappa(r,\theta,\delta)|^{\lambda}} \tag{15}$$

where constants $\beta > 0$ and $\lambda > 1$ are design parameters. Effect of design parameters are illustrated in Fig. 6

For the experiment in section V parameter values $\beta = 0.4$ and $\lambda = 2$ were used, with which $v(\kappa) \simeq 0.4\, v_{\max}$ at $\kappa = 2$, i.e., when the radius of osculating circle is 0.5m.

Then the angular velocity simply follows (13), that is, $\omega = \kappa v$ with v given by (15). With given parameters analytic maximum for angular velocity becomes $\omega_{\max} = \frac{\pi}{4}\, v_{\max}$.

B. Heterogenous Control and Human-like Driving Strategy

When presented with a single target, the control law (13) augmented with (15) allows the vehicle to navigate gracefully. But to navigate in more structured environment, multiple intermediate targets become necessary to reach a goal without collision. Then transitioning between targets becomes an inherent problem, since target switching introduces discontinuity in vehicle state $(r,\theta,\delta)^T$, which may render derivatives of command signals arbitrarily large if the transition is instantaneous. Resulting high acceleration and jerk can lead to actuator overload (thus failure to execute a path) and discomfort to passengers.

Before we proceed further, let us briefly examine how human drivers navigate in an environment. When a human driver approaches a corner, the driver first examines how sharp the turn is and then reduces linear speed accordingly. At the corner, the driver would fix the linear velocity and change angular velocity smoothly to acquire desired heading, and then regain speed after passing the corner and the heading is stabilized. Considering how well a human driver can perform the task, it makes sense to adopt a similar procedure.

Given two consecutive targets $P_i = (r_i, \theta_i, \delta_i)^T$ and $P_{i+1} = (r_{i+1}, \theta_{i+1}, \delta_{i+1})^T$, we first slow down to a desired speed v_{T_i} before reaching P_i. The transition (analogous to turning a corner) is initiated at some threshold distance r_t away from P_i and lasts for a nonzero time interval τ_ω, so that the size of the derivatives become manageable. During the transition linear velocity is held constant and angular velocity transitions from initial angular velocity ω_r to $\omega = \kappa(P_{i+1}) \cdot v_{T_i}$. Finally, the vehicle will speed up again from v_{T_i} to $v(P_{i+1})$, following (15).

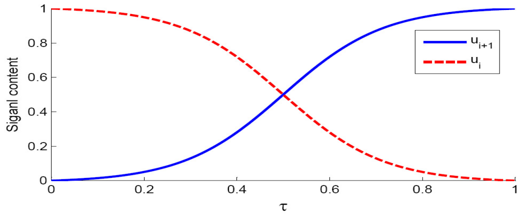

Fig. 7. Change in the signal content under (17), between two heterogeneous signals u_i and u_{i+1} during the transition period τ.

For actual transition, we have developed a heterogeneous control scheme which is a variant of a method proposed in [8]. The idea is to gradually mix two heterogeneous control signals over transition interval τ, using a modified sigmoid function $\sigma_\tau(t)$ which is truncated and rescaled to domain $[0,\tau]$ and range $[0,1]$:

$$\sigma_\tau(t) = \frac{1}{0.98}\left(\frac{1}{1+e^{-9.2(t/\tau-0.5)}} - 0.01\right) \tag{16}$$

Then the mixed signal during the transition from u_i to u_{i+1} is simply given by

$$u(t) = (1-\sigma_\tau(t))\, u_i + \sigma_\tau(t) \cdot u_{i+1} \tag{17}$$

where $t \in [0,\tau]$ is a variable indicating the progress of transition. Fig. 7 shows the change in the signal content using the heterogeneous control.

It can be shown higher derivatives of (17) linearly depends on the magnitude of $\Delta u \equiv u_i - u_{i+1}$. In the proposed scenario, the magnitude of change in angular velocity command $\Delta\omega$ during the transition linearly depends on v_{T_i} since $\omega = \kappa v$. Thus v_{T_i} is an effective handle for the magnitude of the control signal ω and its higher derivatives. Desired linear velocity v_{T_i} given user-specified bounds can easily be obtained numerically via model predictive simulation.

The process can be formally described as forming a motion target $T_i \equiv (P_i^T, v_{T_i})^T$, which is a set of desired linear velocity and target pose in space, by assigning desired linear velocity v_{T_i} to the target pose P_i based on the relationship between P_i and P_{i+1} under (13). Note that the process can be automated and does not require additional input from the user.

V. Results

The proposed control law and the path following algorithm was tested on a physical robot (Fig. 8). The testbed is a differentially driven wheelchair robot equipped with a laser range finder and an IMU, about 1.2m in length and 0.76m in width. Path instructions were given manually by specifying multiple target poses on a map generated via SLAM.

A trajectory of the robot from a typical test run is shown in Fig. 8. The trajectory shown consists of a slow turn (lane change), a 90 degree turn and a final stop, typical actions

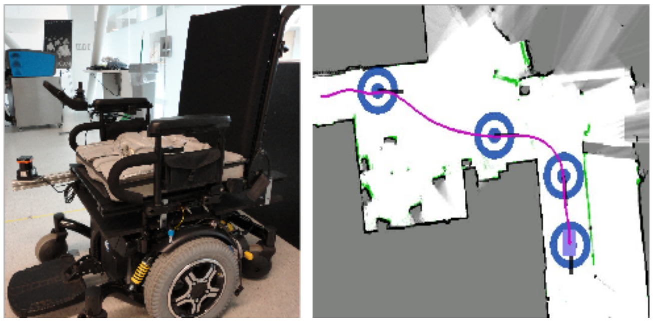

Fig. 8. Left: Differentially driven wheelchair robot. Right: Robot trajectory, traversing distance of 16.7m in 22.3 seconds. Motion targets are marked as concentric circles with protruding line segment indicating target orientation. Final position of the robot is shown as a purple rectangle.

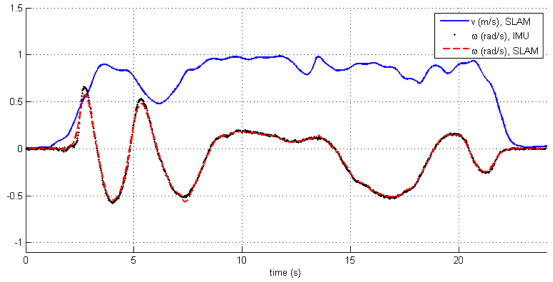

Fig. 9. Linear velocity v and angular velocity ω. Angular velocity measurements from an IMU is also shown. The robot slows down as needed at $t = 4.7, 12.2, 17.1$s, where the target transition occurs. The velocities changes smoothly within imposed bounds. Best viewed in color.

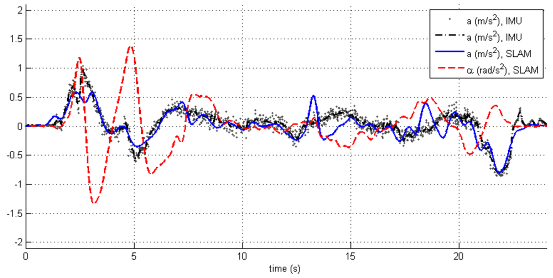

Fig. 10. Linear accleration $a = \dot{v}$, angular acceleration $\alpha = \dot{\omega}$, and linear acceleration measurements from the IMU. Note that the differentiated and smoothed values of a closely tracks the independently measured IMU values. Best viewed in color.

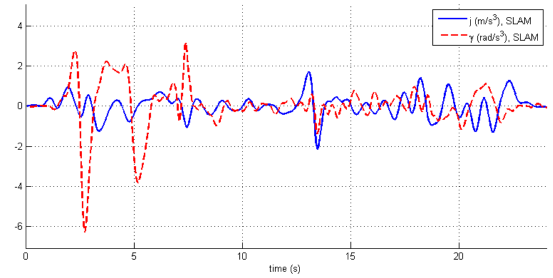

Fig. 11. Linear jerk $j = \ddot{v}$ and angular jerk $\gamma = \ddot{\omega}$, respectively. Both j and γ stays well within the imposed bounds, as can be expected from the smooth trajectory shown in Fig. 8

required to navigate in office environment. Fig. 9 - 11 show the state of the robot along the trajectory.

In the run shown the robot traversed distance of 16.7m in 22.3 seconds. The robot was set to begin slowing down when it reaches the lookahead distance $r_l = 1.5$m from a motion target and commence target transition when it reaches the threshold distance $r_t = 1.0$m (about the size of the robot). The transition lasts over the interval $\tau_\omega = 1.3$s where the blending of angular velocity commands takes place. Numerical values of imposed bounds are $v_{\max} = 1$ m/s, $\omega_{\max} = \frac{\pi}{4}$ rad/s, $\dot{\omega}_{\max} = 2.8\,\text{rad/s}^2$, and $\ddot{\omega}_{\max} = 7.7\,\text{rad/s}^3$, all of which are satisfied over the entire trajectory.

For the implementation, care should be taken to choose appropriate values of threshold distance r_t, since $1/r$ term in the control law (13) can amplify the noise from the localization if v is constant. The issue can be resolved by either setting r_t sufficiently large (for intermediate motion targets) or by letting $v \sim r$, such that $v \to 0$ as $r \to 0$ which cancels each other out (for the final motion target). More data and implementation details will be available in [21].

Data was gathered at 20Hz via SLAM, which give us fairly accurate pose data over the trajectory. Velocity, acceleration and jerk were obtained from the pose data through standard numerical differentiation. To get reliable values for higher derivatives, however, some smoothing operations were necessary, and here local linear regression over a sliding time window of 0.5 second was applied. Since smoothing operations can significantly effect the calculation of the higher derivatives, we also show linear accelerations directly measured at 50Hz from an independent IMU, MicroStrain's *3DM-GX2* [22], for qualitative validation. The shape and the level of the data corresponds well to the calculated value.

VI. Discussion

It is clear that there exists a trade-off between speed/maneuverability and comfort. Here, the curvature based rule for linear velocity (15) and the sigmoid-based heterogeneous control (17) addresses the trade-off by allowing the robot to slow down according to the curvature/discontinuity associated with presented path, by taking advantage of the fact that the smooth control law (13) admits arbitrary linear velocity. The result demonstrates that the presented method can guide the robot quickly and comfortably through multiple motion targets, satisfying the requirement for graceful motion.

Also, we note that the performance of the kinematic control law and the path-following algorithm does depend on its smooth nature. In general, kinematic controller works well only if underlying dynamic controller/actuator is sufficiently fast in achieving reference velocities calculated by the kinematic controller.[5] That is, the derivative of the velocity commands essentially amounts to required torque to satisfy the command. Thus smoothness is necessary for success of pure kinematic controllers.

The approach we are taking is distinct from trying to

[5] See [6] for experimental evaluation of some classical kinematic control laws on a physical robot.

solve the full problem of graceful navigation in a single step (e.g. via global optimization [2]). Here, we are essentially factoring the global navigation problem into two parts: (1) local pose following given the targets in an open space (local navigation and control), and (2) target generation and assignment in a structured and dynamic environment (planning). This work presents a concise and computationally very efficient solution to the local navigation problem of traveling between arbitrary poses quickly and comfortably. Static and dynamic obstacle avoidance will be addressed more explicitly in a near future work for the planning.

VII. Conclusion

The contribution of this paper is the formulation of the kinematic control law (13) and the pose-following algorithm for smooth and comfortable motion of unicycle-type robots.

In section III, we have shown that a natural choice of coordinates and singular decomposition of the system lead to (13) which steers the vehicle to arbitrary motion target in a smooth and intuitive curve. The intuitive nature of the curve renders the trajectory readily acceptable to human passengers, and the characteristic of the path (from pure waypoint following to aggressive pose following) can be easily manipulated via two parameters k_1 and k_2.

In section IV, we have introduced a path following strategy utilizing the fact that the control law admits arbitrary linear velocity. We have also introduced the heterogeneous control scheme which is useful for managing higher derivatives of control signals during target transition. Results show that the vehicle moves gracefully satisfying user-imposed bounds in higher derivatives of control signals, given sparsely placed target poses as path instruction.

The proposed control law and the pose following strategy is important since it provides safety and comfort to user without sacrificing maneuverability, and also avoids actuator overload and makes the path physically realizable.

VIII. ACKNOWLEDGMENTS

The authors would like to thank Zhenghong Sun and Collin Johnson for their aid in implementation of the control algorithm on a physical robot, and Professor Jessy Grizzle for valuable discussions and suggestions.

References

[1] S. Gulati and B. Kuipers, *High Performance Control for Graceful Motion of an Intelligent Wheelchair*, Proceedings of IEEE International Conference on Robotics and Automation, 2008, pp.3932-3938.

[2] S. Gulati, C. Jhurani, B. Kuipers and R. Longoria, *A Framework for Planning Comfortable and Customizable Motion of an Assistive Mobile Robot*, IEEE/RSJ International Conference on Intelligent Robots and Systems, 2009.

[3] M. Breivik and T. Fossen, *Guidance Laws for Planar Motion Control*, Proceedings of 47th IEEE Conference on Decision and Control, 2008, pp.570-577.

[4] K. Konolige, M. Agrawal, R. Bolles, C. Cowan, M. Fischler and B. Gerkey, *Outdoor Mapping and Navigation using Stereo Vision*, Proceedings of International Symposium on Experimental Robotics, 2006.

[5] M. Aicardi, G. Casalino, A. Bicchi, and A. Balestrino, *Closed Loop Steering of Unicycle-like Vehicles via Lyapunov Techniques*, IEEE Robotics and Automation Magazine, vol.2, no.1, pp.27-35, 1995.

[6] B. Kim and P. Tsiotras, *Controllers for Unicycle-Type Wheeled Robots: Theoretical Results and Experimental Validation*, IEEE Transaction on Robotics and Automation, vol.18, no.3, pp.294-307, 2002.

[7] G. Indiveri, A. Nücheter and K. Lingmann, *High Speed Differential Drive Mobile Robot Path Following Control with Bounded Wheel Speed Commands*, Proceedings of IEEE Conference on Robotics and Automation, 2007, pp.2202-2207.

[8] B. J. Kuipers and K. Astrom, *The Composition and Validation of Heterogeneous Control Laws*, Automatica, vol.30, no.2, 1994, pp.233-249.

[9] V. Bakaric, Z. Vukic and R. Antonic, *Improved Basic Planar Algorithm of Vehicle Guidance through Waypoints by the Line of Sight*, First International Symposium on Control, Communications and Signal Processing, 2004, pp.541-544.

[10] A. Aguiar and A. Pascoal, *Dynamic Positioning and Way-Point Tracking of Underactuated AUVs in the Presence of Ocean Currents*, International Journal of Control, vol.80, no.7, pp.1092-1108, 2007.

[11] J. Borenstein and Y. Koren *The Vector Field Histogram - Fast Obstacle Avoidance for Mobile Robots*, IEEE Journal of Robotics and Automation, vol.7, no.3, pp.278-288, 1991.

[12] D. Fox, W. Burgard and S. Thrun, *The Dynamic Window Approach to Collision Avoidance*, IEEE Robotics and Automation Magazine, vol.4, no.1, pp.23-33, 1997.

[13] E. W. Weisstein, *Archimedean Spiral*, From MathWorld–A Wolfram Web Resource.
http://mathworld.wolfram.com/ArchimedeanSpiral.html.

[14] H. Khalil, *Nonlinear Systems, 3rd ed.*, Prentice Hall, Upper Saddle River, NJ, 2002.

[15] S. LaValle, *Planning Algorithms*, Cambridge University Press, New York, 2006.

[16] A. Micaelli and C. Samson, *Trajectory Tracking for Unicycle-Type and Two-Steering Wheels Mobile Robots*, INRIA, Sophia-Antipolis, Tech. Rep. 2097, 1993.

[17] L. Lapierre, D. Soetanto, and A. Pascoal, *Nonsingular Path Following Control of a Unicycle in the Presence of Parametric Modeling Uncertainties*, International Journal of Robust Nonlinear Control, pp.485-503, 2006.

[18] A. Piazzi and C. Bianco, *Quintic G^2-splines for Trajectory Planning of Autonomous Vehicles*, Proceedings of IEEE Intelligent Vehicle Symposium, 2004, pp.620-625.

[19] E. Magid, D. Keren, E. Rivlin, and I. Yavneh, *Spline-Based Mobile Robot Navigation*, Proceedings of the IEEE/RSJ International Conference on Intelligent Robots and Systems, 2006, pp.2296-2301.

[20] R. W. Brockett, *Asymptotic stability and feedback stabilization*, In Differential Geometric Control Theory, pp. 181-191, R. W. Brockett, R. S. Millman, and H. J. Sussmann (Eds.), Boston, Birkhauser, 1983.

[21] J. Park, *Technical Report: Control Algorithm for Graceful Motion and its Implementation*, http://www.eecs.umich.edu/ kuipers/research/

[22] MicroStrain, 3DM-GX2, http://www.microstrain.com/3dm-gx2.aspx